


Article

Experimental Study on the Current Pretreatment-Assisted Free Bulging of 304 Stainless Steel Sheets

Jinchao Sun ¹, Gui Wang ¹, Qingjuan Zhao ^{1,*}, Jiafang Pan ¹, Yunfei Qu ² and Yongxiang Su ¹

¹ Key Laboratory of Advanced Manufacturing and Automation Technology (Guilin University of Technology), Education Department of Guangxi Zhuang Autonomous Region, Guilin 541006, China; 2020155@glut.edu.cn (J.S.); 13462675056@163.com (G.W.); panjiafang@glut.edu.cn (J.P.); 13471360502@163.com (Y.S.)

² School of Light Industry, Harbin University of Commerce, Harbin 150028, China; quyunfei@hrbcu.edu.cn

* Correspondence: tgyx08310@163.com; Tel.: +86-187-6203-7637

Abstract: In order to further improve the microplastic deformation ability and forming performance of metal sheets, a pulse current pretreatment-assisted micro-forming method was proposed. Firstly, a 304 stainless steel sheet was pretreated with current (0–25 A), and the microstructure changes in the sheet under the action of current were analyzed. Then, a current-assisted bulging experiment was carried out from three aspects as follows: current size, mold structure size, and material properties, to explore the influence of different process parameters on the micro-bulging of the sheet. Finally, the forming quality was analyzed and evaluated from the two perspectives of bulging depth and wall thickness uniformity. The research results show that when the current intensity increases from 0 to 25 A, the fibrous distribution in the thickness direction of the sheet is alleviated, the structure is more uniform, the bulging depth shows an increasing trend, and the thinning rate and wall thickness uniformity are improved. When the current intensity reaches 25 A, the bulging depth increases from the original 463 μm to 503 μm , and the thinning rate drops from the most serious 48.52% to 19.4%. At the same time, as the mold size increases, the single-channel aspect ratio (W/H) also increases accordingly. When the mold groove width (W) is 2 mm, the ratio reaches 0.4, the sheet deforms significantly, and the filling effect is better. In addition, the larger the roundness of the convex and concave molds, the more uniform the wall thickness distribution of the bulging parts. Under the same experimental conditions, the bulging depth of the 304 stainless steel sheet is higher than that of TC4 titanium alloy, and it is less prone to springback and is more conducive to plastic deformation.

Keywords: pulsed current; 304 stainless steel sheet; single channel; free bulging



Citation: Sun, J.; Wang, G.; Zhao, Q.; Pan, J.; Qu, Y.; Su, Y. Experimental Study on the Current Pretreatment-Assisted Free Bulging of 304 Stainless Steel Sheets. *Appl. Sci.* **2024**, *14*, 5502. <https://doi.org/10.3390/app14135502>

Academic Editor: Anming Hu

Received: 10 May 2024

Revised: 20 June 2024

Accepted: 22 June 2024

Published: 25 June 2024



Copyright: © 2024 by the authors. Licensee MDPI, Basel, Switzerland. This article is an open access article distributed under the terms and conditions of the Creative Commons Attribution (CC BY) license (<https://creativecommons.org/licenses/by/4.0/>).

1. Introduction

Because of the advancement of science and technology and the needs of production and life, the application of micro-components is becoming more and more widespread, making product micromation a mainstream development trend. At the same time, micro-manufacturing technology has also attracted increasing attention. The industrialization of microsystem technology (MST) and microelectromechanical systems (MEMSs) has greatly promoted the development of microfabrication technology. Ultra-precision machining, deep reactive ion etching, micro-EDM, and rapid prototyping have successively appeared. Although these processing technologies meet the needs of some miniaturized products, they cannot meet the requirements of large production batches, low costs, and high processing accuracy. These requirements limit the wide application of micro-processing technology, which also promotes the rapid development of micro-forming technology.

Plastic micro-forming technology is a method that uses plastic forming to prepare parts with characteristic dimensions reaching sub-millimeter levels in at least two dimensions [1]. Compared with traditional micro-manufacturing technology, it has the advantages of high production efficiency, easy manufacturing, wide processing range, and high product

mechanical properties, making it a very promising micro-parts manufacturing method [2–4]. As a type of plastic micro-forming, thin plate micro-forming technology not only has the advantages of high efficiency and low cost, but it also retains the simple characteristics of traditional plastic processing technology and has broad application prospects in the MEMS field [5]. Commonly used methods in thin plate micro-forming include stretching, bulging, bending, etc. The thin plate micro-bulging process has good applications in small parts because of its advantages of small rebound and high dimensional accuracy. The forming principle relies on a bulging mold to force the sheet to reduce its thickness and increase its surface area under pressure, thereby obtaining corresponding parts. However, the biggest problem in the micro-bulging process is that the thickness is thinned or even cracked during the forming process [6], especially when the size reaches the sub-millimeter level, which is more prominent and directly affects the quality and accuracy of the forming [7].

In response to this problem, domestic and foreign scholars have conducted a considerable amount of research. Sasawat Mahabunphachai et al. [8,9] studied the impact of size effects on micro-feature structure chips during the forming process by performing experiments on the hydraulic micro-bulging of sheets. Olayinka et al. [10] studied the surface roughness of 304 stainless steel foil during micro-bulging through hydraulic micro-bulging experiments. They found that the roughness increased with the increase in strain during bulging and the deformation and induced roughness followed a linear relationship at both the microscale and macroscale. Sun Lijun et al. [11] numerically simulated the micro-bulging of ultra-thin stainless steel sheets and used Hill's concentrated instability theory to predict the rupture limit of the bulging of the sheets.

In recent years, pulsed current-assisted micro-forming technology has gradually emerged. Under the action of pulsed current, materials can reduce flow stress and improve plastic deformation ability, thereby improving the forming effect. Lee et al. [12] conducted a pulse current-assisted V-shaped bending test on AZ31B magnesium alloy plates. Compared with traditional room temperature V-shaped bending, introducing current could effectively reduce springback. As the current density increased, the degree of springback reduction also increased. Liu et al. [13] found that the wall thickness of SiC/Al alloy after electric thermal bulging was thinner than that after ordinary thermal bulging, which showed that electric pulse improved the alloy bulging performance. Fan Rong et al. [14] conducted research on the pulse current-assisted micro-rolling process and quickly produced fine textures on the surface of the part. It has been proven that pulse current can increase the depth and width of surface grooves and improve the surface quality. However, the application of pulse current to micro-bulging of metal sheets is currently less studied.

Because of the thin size of metal sheets and severe work hardening, the traditional bulging method is to use a heat treatment strengthening process to improve the various properties of a sheet and then bulge. However, this method is not only inefficient but also needs to consider the oxidation problem of metal materials. In view of this, applying pulse current pretreatment to a sheet can quickly heat it in a short time to eliminate work hardening and improve the forming performance of the sheet, which is a new strengthening treatment process. In recent years, pulsed current technology has been considered an alternative to heat treatment [15–18]. In general, pretreatment-assisted forming with the help of a pulse current is a green and efficient micro-forming method; it has great potential in the manufacturing of materials with poor plasticity that are difficult to deform.

Therefore, in order to solve the problems of serious thinning and poor forming quality in the micro-bulging process, this paper combines pulse current technology with the micro-bulging process. It also extends free-bulging experiments by performing current pretreatment with different process parameters on 304 stainless steel sheets to explore new methods that can improve the quality of the micro-bulging of metal sheets.

2. Experimental Procedure and Mold Design

In this experiment, a cold-rolled 304 stainless steel sheet with dimensions of $150 \times 20 \text{ mm} \times 0.1 \text{ mm}$ was selected as the current pretreatment-assisted free bulging material,

and TC4 titanium alloy was used as the comparison material. Its chemical composition is shown in Table 1. Before conducting the bulging experiment, a pulse current pretreatment experimental platform was independently built. The current pretreatment platform is shown in Figure 1. The platform consists of a pulsed power supply and a treatment device. The treatment device includes a metal sheet, a baseplate, pressing plates, clamps, and electrodes. The baseplate is made of high-temperature resistant asbestos board, and the pressing plates are made of ceramic fiber material, which can withstand high temperatures and play an insulating role. The clamps are used to hold the sheet. A T2 copper sheet with a thickness of 3 mm was used as electrodes to achieve rapid current transmission. The 304 stainless steel sheet was pretreated using the current pretreatment platform. The pulse current parameter information is shown in Table 2. In order to prevent the metal sheet from oxidizing, a layer of boron nitride paint was coated on its surface. At the same time, an infrared thermometer gun was used to monitor the temperature changes in the sheet in real time. Finally, the pretreated material was cut into 20×20 mm square blanks for micro-bulging, as shown in Figure 2.

Table 1. Chemical composition of 304 stainless steel and TC4 titanium alloy (wt%).

Material	Element Content							
	C	Si	Mn	P	S	Ni	Cr	Fe
304 stainless steel	0.08	0.75	2	0.045	0.03	8~10.5	18~20	Bal
TC4 titanium alloy	Al	V	Fe	C	H	O	Ti	
	5.917	4.614	0.115	0.005	0.008	0.071	Bal	

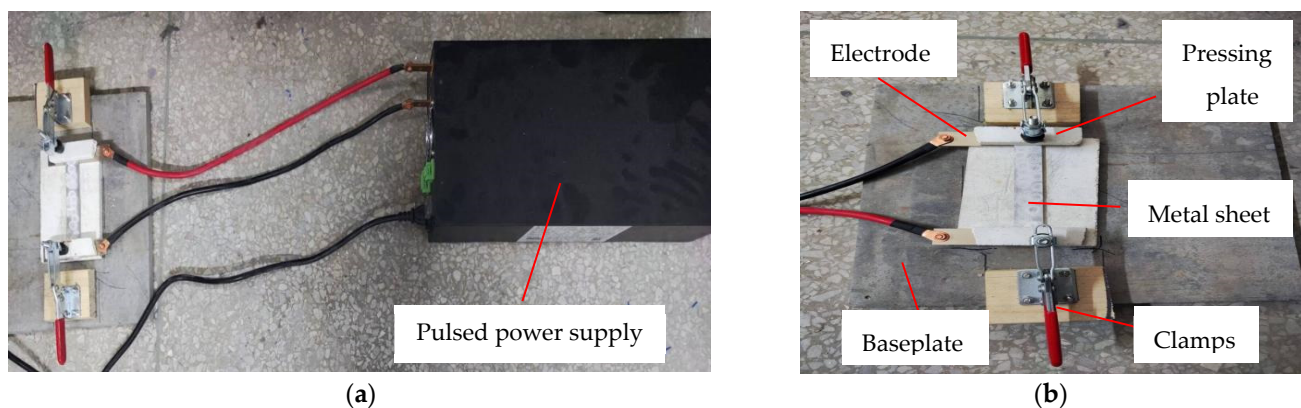


Figure 1. Current pretreatment platform. (a) The pulse power supply used to provide current. (b) The treatment device used for current pretreatment.

Table 2. Pulse current pretreatment parameters.

Serial Number	Current Strength/A	Pulse Frequency/Hz	Processing Time/s	Duty Ratio/%	Temperature/°C
1	/	/	/	/	25
2	10	50	120	50	50
3	15	50	120	50	75
4	20	50	120	50	110
5	25	50	120	50	150

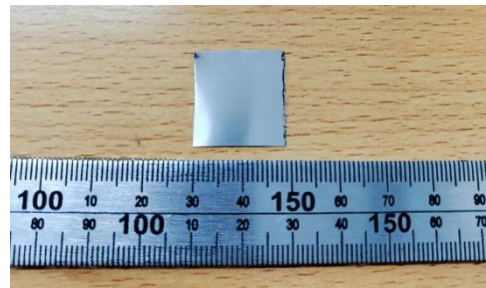


Figure 2. Square blanks.

The micro-bulging experimental device consists of a pressure-loading device and a bulging mold. The pressure-loading device uses an SK-3T three-plate and four-column pneumatic press. The various process parameters are shown in Table 3.

Table 3. Press parameters.

Parameter	Maximum Theoretical Output/kg	Air Source Range/Mpa	Rated Voltage/V	Effective Size/mm
Value	3000	0.4–0.7	220	350 × 300 × 240

Since the pneumatic press relies on gas to transmit pressure, an external air source device was required. An air compressor capable of supplying 0.7 MPa was selected based on the requirements of the suitable air source range. The whole pressure-loading device is shown in Figure 3.



Figure 3. Pressure-loading device. (a) Pneumatic press. (b) Pressure-loading device.

The bulging mold is the core of micro-forming. On the one hand, it must be accurately connected to the press, and on the other hand, it must ensure the mold closing accuracy of the upper and lower molds. This article uses traditional rigid mold micro-bulging. The mold is shown in Figure 4, which mainly consists of the upper and lower templates, convex and concave molds, pillars, washers, and several parts. The entire mold adopts an inlaid design, and the mold base is fixed. The convex and concave molds are replaced with different sizes to bulge parts of different sizes. The forming principle relies on the press to provide pressure to complete the closing of the convex and concave molds, causing the material to deform plastically in the mold to form micro parts. The experimentally designed single-channel convex and concave mold is shown in Figure 5. The main parameters of the single channel include groove width, groove depth, and fillet. Three sets of convex and concave molds of different sizes are used in this article. The ratio of the groove width to groove depth satisfies 2:1 to analyze the influence of mold size on bulging. The geometric parameters are shown in Table 4.

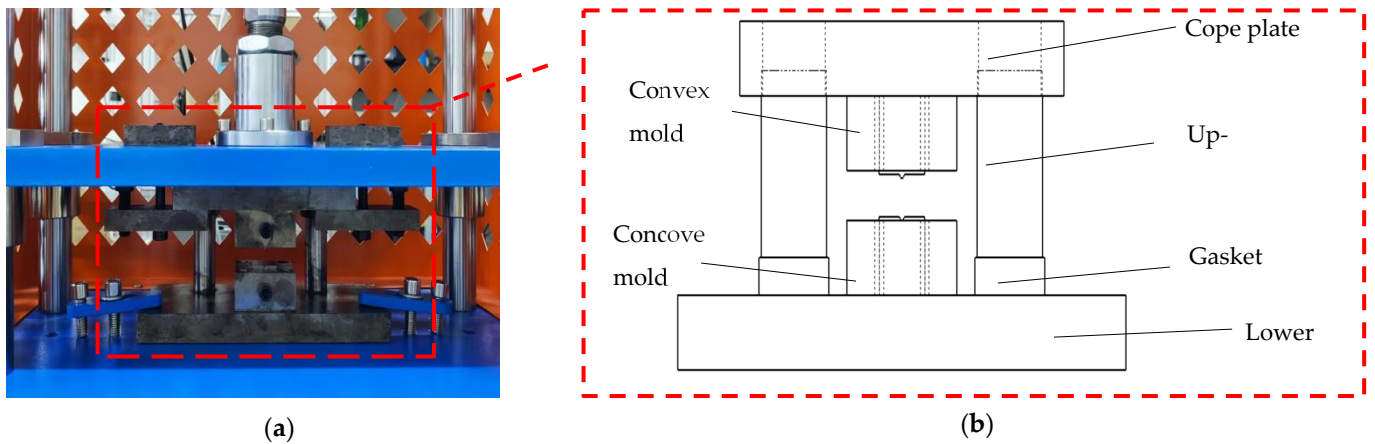


Figure 4. Micro-bulging mold. (a) Physical drawing of the mold. (b) Drawing of the mold structure.

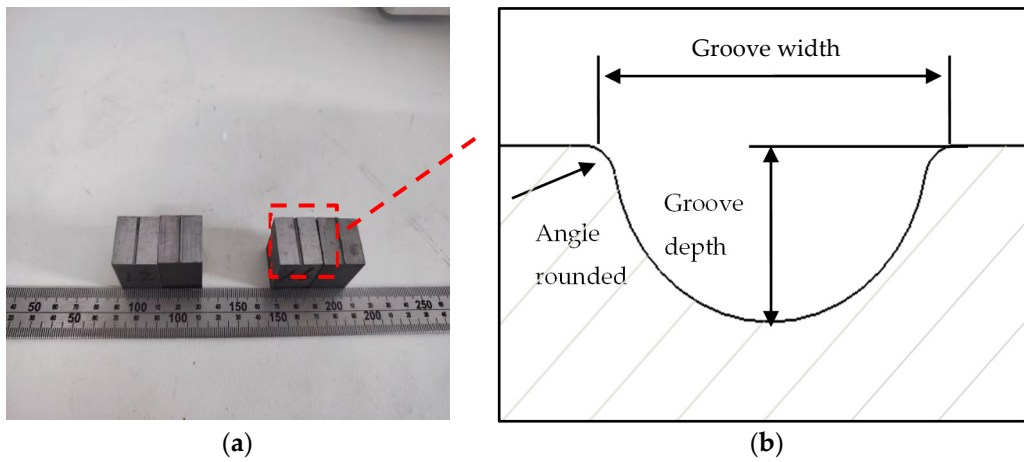


Figure 5. Single-channel convex and concave molds. (a) Physical diagram of the convex and concave molds. (b) Single-channel shape structure.

Table 4. Single-channel mold geometry.

Mold Form	Groove Width, W/mm	Groove Depth, H/mm	Rounded Angle, Ra/mm
convex mold	1.2	0.6	0.12
	1.6	0.8	0.16
	2	1	0.2
concave mold	1.2	0.6	0.12
	1.6	0.8	0.16
	2	1	0.2

Since the parts to be formed reach the micron level, high requirements are placed on the plastic deformation ability of the material. This article first pretreats the 304 stainless steel sheet by applying different intensities of a pulse current and analyzes the microstructure changes in the sheet under the action of the current. It then conducts current-assisted bulging experiments from three aspects, including current size, mold structure size, and material properties, to explore the influence of different process parameters on the micro-bulging of the sheets. The experimental plan is shown in Table 5. The formed micro-bulging parts were cold-mounted, ground, and polished, and the geometric dimensions of the formed single-channel micro-groove were measured using a 4XC metallographic microscope (OM). Each set of experiments was performed three times, the average value

was taken, and the forming effect was analyzed and evaluated for quality in terms of the depth of the bulging and the uniformity of the wall thickness.

Table 5. Experimental scheme of micro-bulging.

Experimental Group Number	Experiment Parameter
Group 1 (current size)	0 A
	10 A
	15 A
	20 A
	25 A
Group 2 (mold size)	groove width/W 1.2 mm groove depth/H 0.6 mm
	groove width/W 1.6 mm groove depth/H 0.8 mm
	groove width/W 2 mm groove depth/H 1 mm
Group 3 (material properties)	304 stainless steel
	TC4 titanium alloy

3. Results and Discussion

3.1. Pulse Current Pretreatment

According to the current parameter information, pulse currents of different intensities (10 A, 15 A, 20 A, 25 A) were applied to the 304 stainless steel sheet for pretreatment. The processing time was 2 min. Under the action of the current, the sheet was heated rapidly in a short time by self-resistance heating. The initial temperature of the rolled sheet was 25 °C. During the heating process, the surface temperature was measured every 5 s using an infrared temperature measuring gun. The temperature rise curve of the sheet after different current treatments was obtained, as shown in Figure 6.

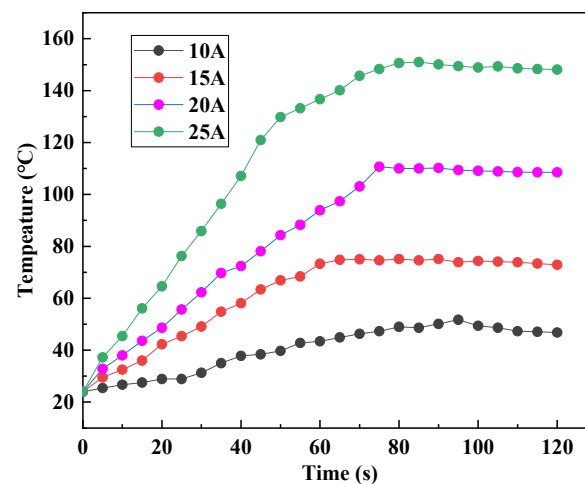


Figure 6. Temperature rise curves of 304 stainless steel sheets after pulsed current treatment with different strengths.

It can be seen from the figure that in the initial stage of current heating, the temperature showed a linear upward trend. The greater the current intensity, the faster the heating rate, which conforms to the Joule heat law of current. The temperature rise change in current heating can be expressed as [19]:

$$\Delta T = \frac{\rho j^2 t}{C_p d} \quad (1)$$

where ΔT is the temperature rise, P is resistivity, j is the pulse current density, t is the pulse treatment time, C_p is the specific heat capacity, and d is the material density. As the current continues to heat, the temperature rise rate gradually slows down, and, finally, the

heating temperature of the thin plate tends to stabilize. This phenomenon occurs because the energy generated by the current and the energy dissipated tend to stabilize, and the temperature of the stainless steel thin plate reaches a dynamic equilibrium state. After being treated with currents of different intensities, the temperature of the thin plate reached about 50 °C, 75 °C, 110 °C, and 150 °C, respectively. The thin plate heated by the current was cooled at room temperature.

3.2. Influence of Pulsed Current on the Microstructure of 304 Stainless Steel Sheet

Metallographic microanalysis of the initial rolling state and different current-treated 304 stainless steel sheets was used to explore the changes in microstructure in the thickness direction of the 304 stainless steel sheet after pulse current treatment. Figure 7 shows the microstructure of the 304 stainless steel sheet in different states, and Figure 7a shows the microstructure of the stainless steel sheet in the original rolling state. It can be seen that the initial 304 stainless steel sheet underwent a large extrusion deformation because of the cold rolling process, and the grains in the thickness direction were destroyed and elongated along the rolling direction. The microstructure shows a fibrous distribution, with high density of dislocations and stress concentration inside, resulting in increased hardness and yield strength and serious work hardening. When subjected to external forces, the deformation between the grains is not coordinated, it is difficult to undergo plastic deformation, and the forming performance is poor.

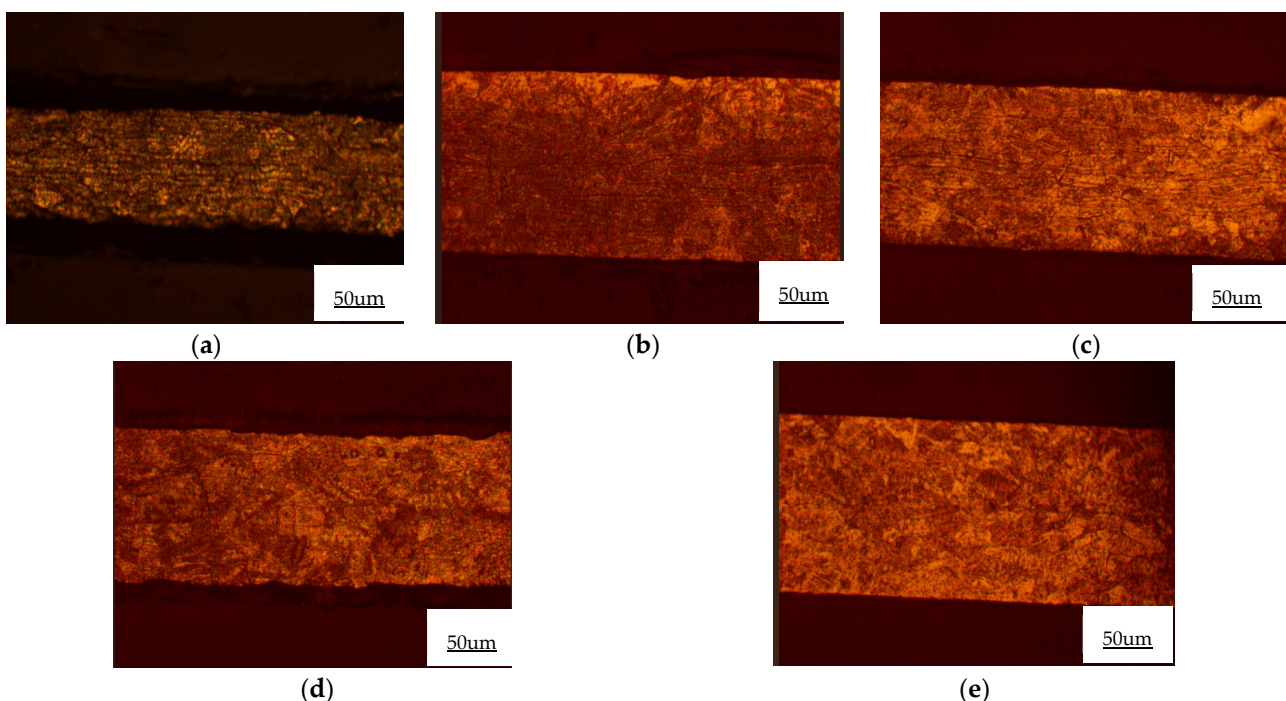


Figure 7. Microstructure changes in 304 stainless steel sheets after treatment with different intensity currents. (a) Rolled state; (b) 10 A; (c) 15 A; (d) 20 A; and (e) 25 A.

Figure 7b is a microstructure diagram of the 304 stainless steel sheet after 10 A pulse current treatment. It can be observed that the fibrous distribution was alleviated and the microstructure began to become uniform. As shown in Figure 7e, under the action of the pulse current (25 A), the internal microstructure underwent dynamic recovery, equiaxed austenite grains appeared, and the grain morphology gradually emerged, which shows that the pulse current promotes coordinated deformation among grains, reduces the dislocation density, and reduces work hardening. During the forming process, this is more conducive to the plastic deformation of the sheet and improves its forming performance.

3.3. Influence of Pulse Current on 304 Stainless Steel Sheet Bulging

The 304 stainless steel plate was treated with different current sizes (0, 10, 15, 20, 25 A), and the convex and concave molds with a slot width of 1.6 mm and a slot depth of 0.8 mm were used to carry out the free bulging experiments under the conditions of a pressure of 0.5 Mpa and a holding time of 1.5 s. The formed bulging parts are shown in Figure 8.

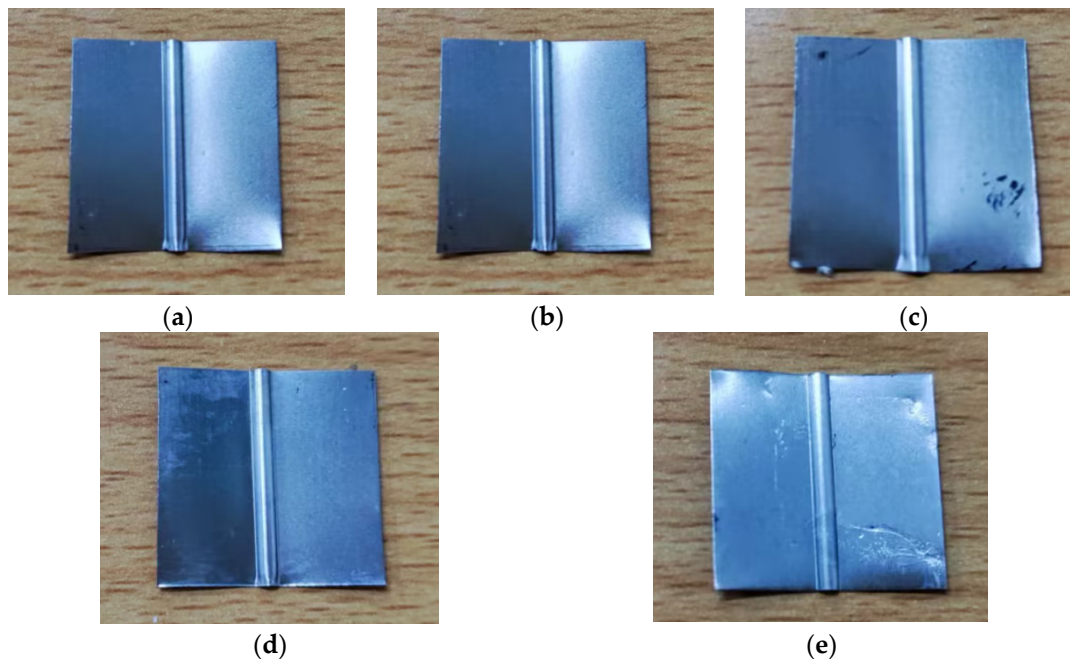


Figure 8. Physical diagram of the bulging of 304 stainless steel sheets with different current sizes. (a) Rolling state; (b) 10 A; (c) 15 A; (d) 20 A; and (e) 25 A.

Under different current sizes, the bulging depth of the stainless steel sheet is shown in Figure 9, and it can be seen from the figure that the bulging depth of the rolled sheet without current application is only 464 μm . After the application of current treatment, the bulging depth shows a gradual increase in the trend of the bulging depth. When the current is 10 A, the bulging depth is about 476 μm , which is an increase of about 2.6% compared with the rolled state. When the current is 15 A, the bulging depth is about 482 μm , which is an increase of about 3.9% compared with the rolled state. When the current is 20 A and 25 A, the bulging depth is 491 μm and 503 μm , which increases by 5.9% and 8.4%, respectively. According to the research of Harvey [20], during the plastic deformation process of the sheet, its flow stress and dislocation satisfy the following relationship:

$$\sigma = \sigma_0 + \alpha Gb\sqrt{\rho} \quad (2)$$

where σ_0 is the flow stress without work hardening, α is a constant, G is the shear modulus, b is the Berthold vector, and ρ is the dislocation density. Since the rolled stainless steel sheet undergoes large strain deformation, there are a large number of dislocation entanglements and martensite transformation inside it, which seriously hinders the slip and climb of dislocations and causes the flow stress to increase during the bulging process of the sheet. At the same time, the degree of plastic deformation is small, and the bulging depth is low. Compared with the rolled sheet, after the stainless steel sheet is treated with the appropriate pulse current, under the coupling effect of the Joule heating effect of the current, and the electron wind force, the dislocation density inside the sheet is significantly reduced and the martensite undergoes dynamic recovery, which reduces the flow stress. During bulging, large plastic deformation can occur, and the bulging depth increases. In addition, the inertial effect also has a certain impact on the bulging depth. The inertial effect means

that when the external load on the material disappears, it will continue to deform and move. Research by Qi et al. [21] shows that microscopic cracks inside the material will cause the inertia effect to weaken. However, under the action of pulse current, the material will generate thermal compressive stress at the microcracks, which promotes the healing of microcracks and micropores [22]. With the reduction in microcracks, the inertial effect of the material is enhanced, thereby improving the plasticity and increasing the depth of bulging.

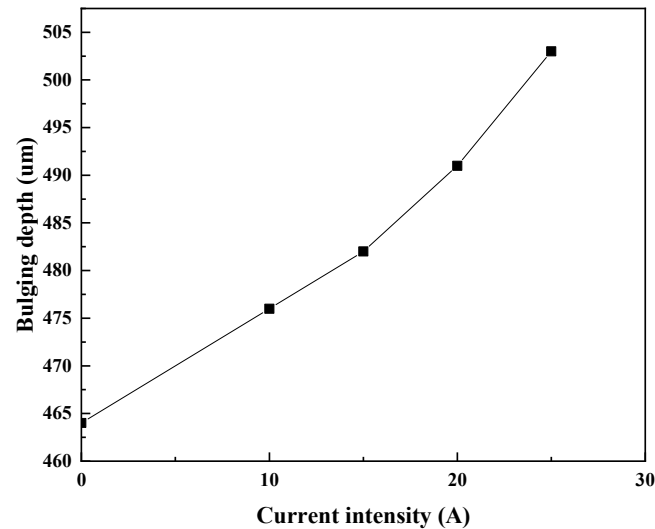


Figure 9. Bulging depth of the 304 stainless steel sheet with different current sizes.

Since the formed single channel is a symmetrical shape, 10 positions of half of the formed section are taken for wall thickness measurement, and the wall thickness measurement positions are shown in Figure 10. Each position was measured five times, and the average value was taken. The thickness change in the forming section is expressed by using the thinning rate, and the formula of the thinning rate can be calculated by the following formula:

$$T = \frac{t_0 - t_i}{t_0} \times 100\% \quad (3)$$

where t_0 is the thickness of the sheet before forming and t_i is the thickness at the measurement point after forming.

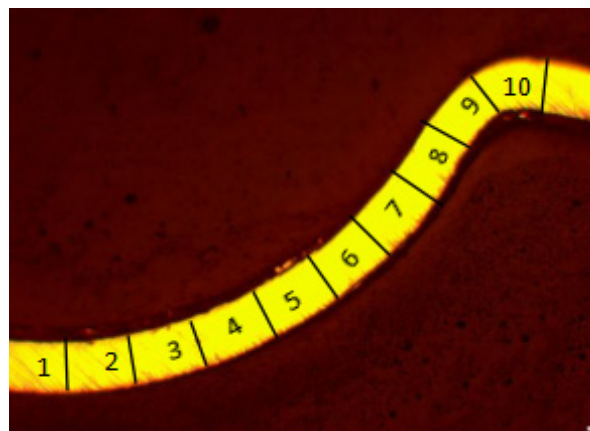


Figure 10. Schematic diagram of measuring position of wall thickness.

Figure 11 shows the wall thickness distribution and thinning rate of the sheet after forming under different current intensities. Through observation, it can be found that the

thickness distribution of the rolled sheet shows great unevenness, and the thinning is the largest at position 9. The thinning rate reached about 48.52%. In addition to position 9, there is also relatively serious thinning at the transition positions of the fillets at 6, 7, and 8. This shows that during the free bulging process, the sheet deforms first at the rounded corners and then gradually flows into the entire mold cavity along with the rounded corners to complete plastic deformation. Significant necking occurs at the rounded corners, resulting in a high rate of thinning. Since position 10 is the first to contact the convex and concave molds during the bulging process, it cannot move under the action of the edge force of the convex and concave molds and is in a stagnant state. Therefore, the wall thickness remains basically unchanged and the thinning rate is low. From positions 1 to 5, the wall thickness shows a gradually increasing trend. Overall, from positions 1 to 10, the wall thickness shows a pattern of first increasing and then decreasing. After being treated with pulse currents of different intensities, the thinning rate of the formed parts was improved accordingly. The thinning rate at fillet position 9 reduced to 35.81% and 27.07% when the current was 20 A and 25 A, respectively. The entire wall thickness distribution also gradually became uniform, and the formability improved. The shape and size of the internal grains of the material are important factors affecting the uniformity after plastic deformation [23–25]. The internal grains of the cold-rolled sheet are destroyed and distributed in a fibrous shape with severe anisotropy. When subjected to large stamping loads, because of the poor fluidity of the fibrous grains, the necking phenomenon is significant at the fillets, the thinning is high, and the overall thickness distribution is uneven. The pulse current promotes the dynamic recovery of grains, making the structure more uniform and improving fluidity. Therefore, during bulging, the thickness distribution of the entire cross-section is more uniform, the necking phenomenon at the fillets is weakened, and the thinning rate is low.

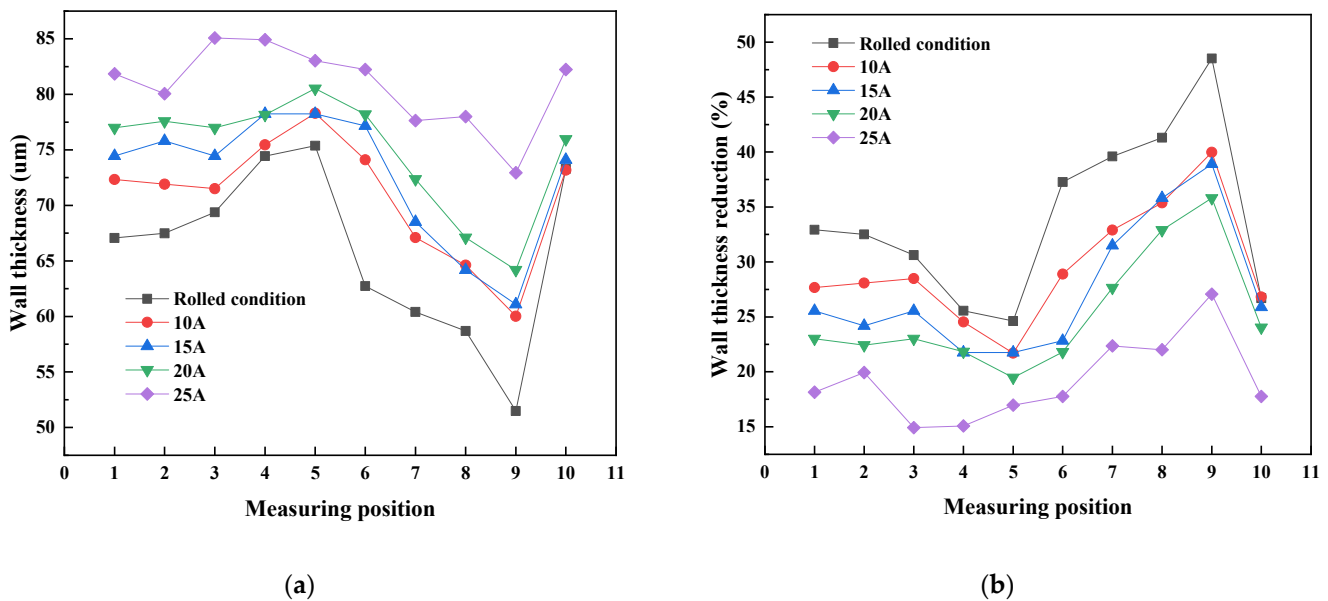


Figure 11. Distribution of the single-channel wall thickness and thinning rate. (a) Wall thickness distribution. (b) Wall thickness thinning rate.

3.4. Influence of Mold Size on 304 Stainless Sheet Bulging

Under the pressure condition of 0.5 Mpa and holding time of 1.5 s, the 304 stainless steel sheet was subjected to 25 A current treatment, and the stainless steel sheet was subjected to bulging experiments using molds with different convex and concave mold sizes (slot width W of 1.2 mm, 1.6 mm, and 2 mm). The specific mold parameters are shown in Table 4. The single-channel bulging parts under different mold sizes are shown in Figure 12. The depth–width ratio of the bulging parts under different mold sizes is shown in Figure 13.

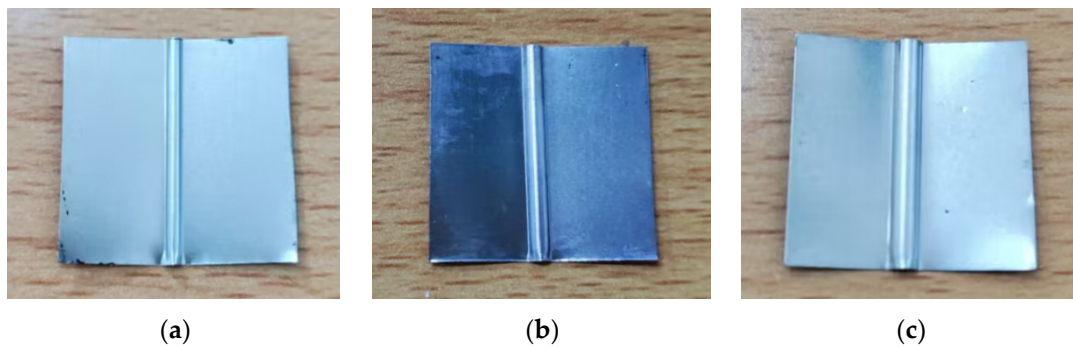


Figure 12. Real picture of the 304 stainless steel sheet formed under different die sizes. (a) Slot width of 1.2 mm; (b) slot width of 1.6 mm; and (c) slot width of 2 mm.

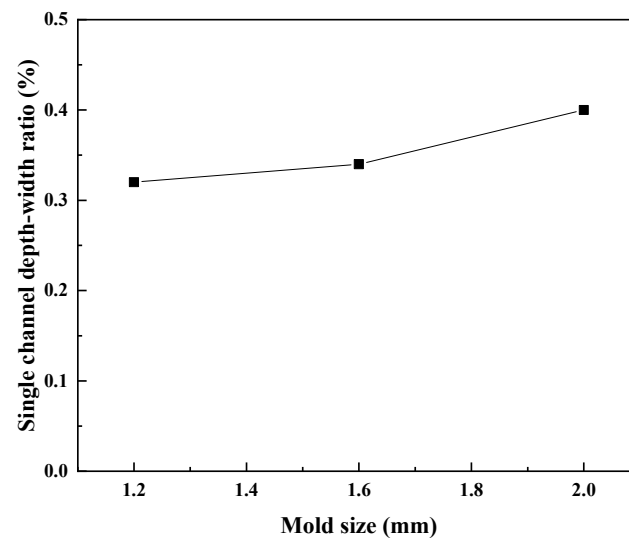


Figure 13. Depth-to-width ratio of the 304 stainless steel sheet for a single channel under different mold sizes.

It can be seen in Figure 13 that the single-channel aspect ratio of the bulging part increases as the mold size increases. When the groove width W of the convex and concave mold is 1.2 mm and the groove depth H is 0.6 mm, the aspect ratio (W/H) of the bulging part is 0.32. When the groove width W of the convex and concave mold is 2 mm and the groove depth H is 1 mm, the aspect ratio (W/H) increases from 0.32 to 0.4, which results in a better filling effect.

This is mainly because the mold cavity size in the bulging process of the material has a certain constraint. The plastic deformation of the sheet is limited to the fixed deformation zone of the convex and concave molds. During the forming process, the sheet on the periphery of the forming area is tightly attached to the surface of the mold under the action of the pressing force F_c , and it does not enter the deformation zone from the outside and the material inside the forming area does not transfer to the outside of the deformation zone. Under the action of the punch pressure load FP and the inertial force, the material in the deformation zone is stretched and thinned because of bidirectional tensile stress (radial stress σ_1 and tangential stress σ_2), and it starts to flow from the rounded corner part to the inside and gradually fills the entire mold cavity, forming a single-channel micro-groove. The bulging principle is shown in Figure 14. Under the same load, when the mold size is smaller, the material inside the convex–concave model cavity is more constrained during the filling process, and flow and plastic deformation are more difficult. Therefore, the depth-to-width ratio of the entire bulging member is small. As the size of the convex–concave model cavity increases, the material flows more easily into the cavity, thereby better completing plastic deformation, and the aspect ratio gradually increases. In addition, during

the forming process, the load on the material per unit area is the same. As the size of the convex and concave molds increases, more materials participate in plastic deformation, which can obtain greater deformation energy and increase the deformation amount of the sheet.

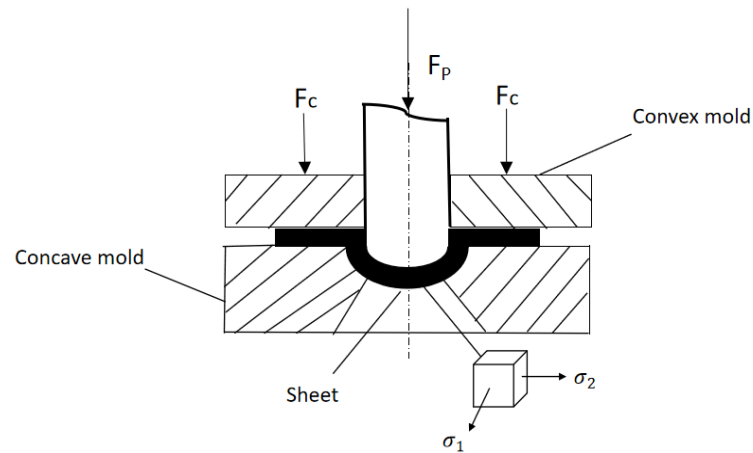


Figure 14. Bulging principle diagram.

The thickness of the stainless steel sheet bulging parts under different mold sizes was measured at different positions, and the wall thickness distribution diagram shown in Figure 15 was obtained. It can be seen in the figure that as the mold size increases, the overall wall thickness distribution of the bulging part becomes more uniform. When the mold size has a groove width W of 2 mm and groove depth H of 1 mm, the thinning rate at fillet position 9 improves significantly and drops to about 19.4%. This is because as the mold cavity size increases, the fillet of the convex and concave molds also increases from the original 0.12 mm to 0.2 mm. The increase in the rounded corners of the convex and concave molds reduces the deformation resistance at the rounded corners of the sheet during the forming process, which significantly improves the material fluidity, thereby maintaining a more uniform wall thickness distribution in various areas. When the rounded corners of the convex and concave molds are small, the flow stress at the rounded corners increases, which easily causes stress concentration, necking, and even rupture, hindering the plastic deformation of the sheet. The overall wall thickness distribution is uneven.

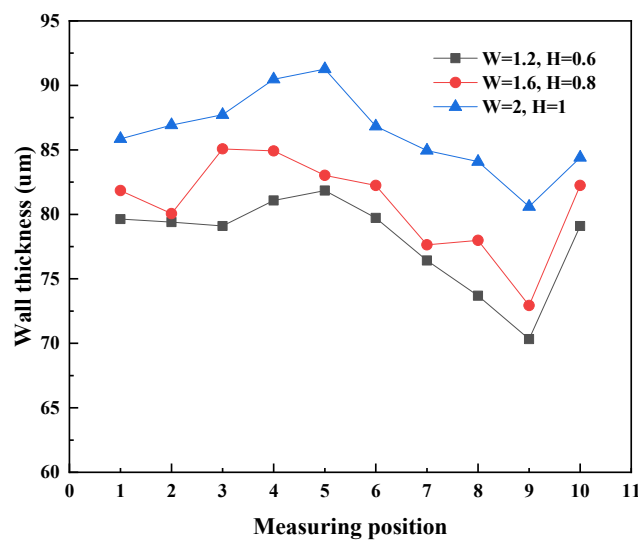


Figure 15. Wall thickness distribution of the 304 stainless steel sheet bulging parts under different mold sizes.

3.5. Influence of Material Properties on 304 Stainless Sheet Bulging

Under the pressure condition of 0.5 Mpa and a holding time of 1.5 s, using a convex and concave mold with a groove width W of 1.6 mm and a depth H of 0.8 mm, a 25 A current was applied to the 304 stainless steel sheet and the TC4 titanium alloy to conduct bulging experiments. The single-channel bulging parts of different materials are shown in Figure 16. Under the same experimental conditions, it can be clearly seen that the bulging parts of the TC4 titanium alloy have obvious rebound phenomenon compared with the 304 stainless steel. This is mainly due to the fact that the elemental component of the TC4 titanium alloy is mainly Al, which is an $\alpha + \beta$ type alloy that has high strength, toughness, and yield strength at room temperature. When subjected to a pressure load, its cold deformation is difficult, and the elastic modulus is small. When the pressure load is removed, large relaxation stress and strain are generated, resulting in obvious bending springback. The 304 stainless steel sample is an austenitic stainless steel with a soft structure, good plastic deformation ability, low yield strength, and large elastic modulus, so there is no obvious rebound phenomenon during the forming process.

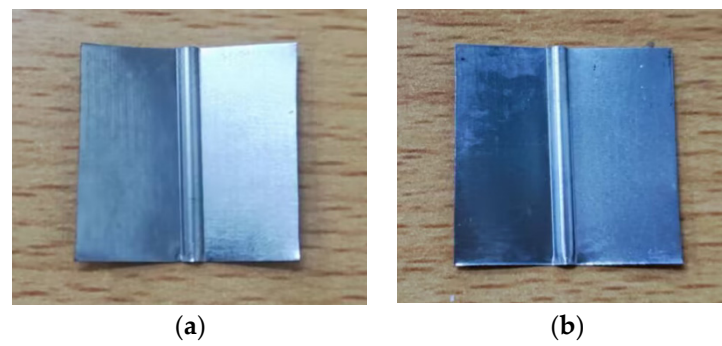


Figure 16. Physical diagram of the bulging parts under different materials: (a) 304 stainless steel; (b) TC4 titanium alloy.

Figure 17 shows the bulging depths of different materials. It can be seen that the bulging depths of the stainless steel sheets and TC4 titanium alloy are 503 μm and 364 μm , respectively. This is mainly due to the lower yield limit of the stainless steel sheets. When performing bulging, the smaller the yield strength, the less energy required for the plastic deformation of the material and the easier it is to form. Under the same external load, the forming effect is better. Therefore, the bulging depth of the 304 stainless steel sheets is relatively high. Another reason is that the resistivities of the two materials are different. Compared with the TC4 titanium alloy, the 304 stainless steel sheet has a larger resistivity and is more sensitive to current, allowing it to generate a higher temperature rise and obtain more Joule heat under the same current. When the current is 25 A, its mechanical properties and microstructure are significantly improved, and the electroplastic effect is obvious.

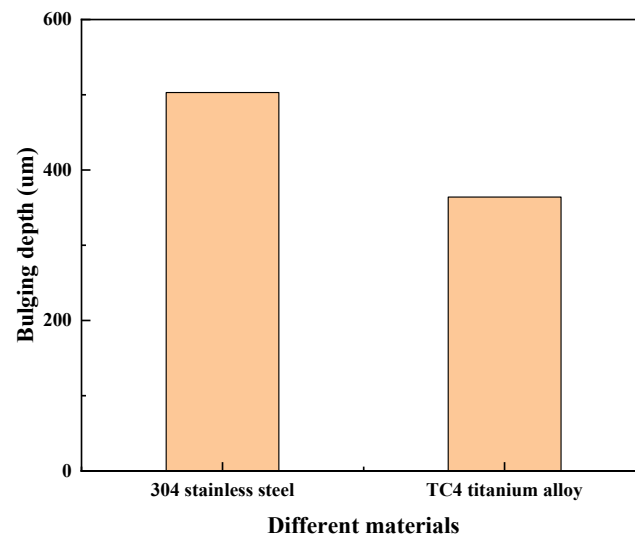


Figure 17. Bulging depth diagram under different materials.

4. Conclusions

The current study shows that the combination of pulsed current and the micro-bulging process can better enhance the forming ability of stainless steel sheets. According to the experimental results, the following conclusions can be drawn:

- (1) After the initial stainless steel sheet is rolled, the grains in the thickness direction are destroyed and present a fibrous distribution, resulting in severe work hardening. After being treated with pulse currents of different intensities, the fibrous distribution in the thickness direction of the sheet is alleviated, and its microstructure is more uniform, which is more conducive to the plastic deformation of the sheet and improves the forming performance.
- (2) As the current intensity increases, the bulging depth of the 304 stainless steel sheet shows a gradually increasing trend, and the thinning rate and wall thickness uniformity are also improved. Compared with the rolled sheet, the bulging depth increases from the original 464 μm to 503 μm when the current is 25 A, and the thinning rate dropped from the most serious 48.52% to 19.4%.
- (3) As the size of the mold increases, the aspect ratio (W/H) of the single-channel bulging part also increases. When the mold micro-groove width W is 2 mm, this ratio reaches 0.4. At this time, the plate deformation is obvious, and the filling effect is good. The larger the rounded corners of the convex and concave molds, the smaller the flow stress at the rounded corners during the forming process, and the more uniform the wall thickness distribution of the bulging parts.
- (4) Compared with TC4 titanium alloy, the 304 stainless steel sheet has higher resistivity under the same experimental conditions, and its electroplastic effect is significant when the current is 25 A. Moreover, it has a high bulging depth and low yield strength, and springback and deformation cannot easily occur, which is more conducive to plastic deformation.

5. Patents

We have applied for a Chinese invention patent for the current pretreatment platform built in this paper and the proposed method of sheet metal micro-forming (Application No. 202410025481.5).

Author Contributions: Conceptualization, G.W., J.S. and Q.Z.; methodology, G.W. and Q.Z.; software, J.S. and G.W.; validation, J.P.; formal analysis, G.W.; investigation, Y.Q. and J.S.; resources, J.S.; data curation, G.W. and Y.S.; writing—original draft preparation, J.S., G.W. and Q.Z.; writing—review and editing, G.W., J.P. and Y.Q.; visualization, Y.S.; supervision, J.S. and G.W.; project administration J.S.

and Q.Z.; funding acquisition J.S. and Q.Z. All authors have read and agreed to the published version of the manuscript.

Funding: This research was funded by the Science and Technology Program of Guang xi, grant number 2021AC19328, and the Project on Electromagnetic Field-Assisted Micro-forming Process and Deformation Mechanism of Titanium Alloy Foil and Plates, grant number 2022KY0260.

Institutional Review Board Statement: Not applicable.

Informed Consent Statement: Not applicable.

Data Availability Statement: The original contributions presented in the study are included in the article, further inquiries can be directed to the corresponding author.

Conflicts of Interest: The authors declare no conflicts of interest.

References

1. Shan, D.B.; Xu, J.; Wang, C.J.; Guo, B. Research progress of plastic microforming technology. *Mater. China* **2016**, *35*, 251–261.
2. Shi, Y.; Zhang, W.; Cao, J.; Ehmana, K.F. Experimental study of water jet incremental micro-forming with supporting dies. *J. Mater. Process. Technol.* **2019**, *268*, 117–131. [[CrossRef](#)]
3. Bansal, A.; Jiang, B.; Ni, J. Die-less fabrication of miniaturized parts through single point incremental micro-forming. *J. Manuf. Process.* **2019**, *43*, 20–25. [[CrossRef](#)]
4. Liu, D.Z. Research status and development trend of thin sheet microforming process. *Sci. Technol. Vis.* **2018**, *35*, 116–118.
5. Zhang, K.F.; Lei, K. Microforming technology for microfabrication. *China Mech. Eng.* **2014**, *12*, 89–95.
6. Zhao, D.; Zhang, M.Y.; Li, G.Z.; Wang, S.B.; Zhang, M.; Li, X.M.; Su, C.J. Effect of plate thickness on forming limit of 08Al sheet in single point progressive forming. *J. Netshape Form. Eng.* **2022**, *14*, 14–19.
7. Xu, Z.T.; Sun, L.; Jiang, T.H.; Peng, L.F.; Lai, X.M. Fracture scale effect and microscopic damage criterion of Titanium plate Micro-forming. *J. Mech. Eng.* **2022**, *58*, 55–57.
8. Mahabunphachai, S.; Koc, M. Fabrication of micro-channel arrays on thin metallic sheet using internal fluid pressure: Investigations on size effects and development of design guidelines. *J. Power Sources* **2007**, *175*, 363–371. [[CrossRef](#)]
9. Mahabunphachai, S.; Koc, M. Investigation of size effects on material behavior of thin sheet metals using hydraulic bulge testing at micro/meso-scales. *Int. J. Mach. Tools Manuf.* **2008**, *48*, 1014–1029. [[CrossRef](#)]
10. Olayinka, A.; Emblom, W.J.; Wagner, S.W.; Khnosari, M.; Haghshenas, A. Investigation of deformation induced micro to macro scale surface roughness. *Procedia Manuf.* **2020**, *48*, 237–243. [[CrossRef](#)]
11. Sun, L.J.; Huang, Z.Y.; Zhang, H.; Ruan, F. Research on prediction theory of expansion rupture limit of ultra-thin plate. *Forg. Stamping Technol.* **2013**, *38*, 142–146.
12. Lee, J.; Bong, H.J.; Lee, Y.S.; Kim, D.; Lee, M.G. Pulsed Electric Current V-Bending Springback of AZ31B Magnesium Alloy Sheets. *Metall. Mater. Trans. A* **2019**, *50*, 2720–2731. [[CrossRef](#)]
13. Zhang, K.F.; Liu, J.Y. Promotion mechanism of electric current on SiC/Al composite material deformation. *Mater. Sci. Technol.* **2015**, *31*, 468–473.
14. Fan, R. Effect of Current on Mechanical Properties of Metal Alloys and its Mechanism. Master's Thesis, Dalian University of Technology, Dalian, China, 2016.
15. Leopold, K.; Anatoly, B.; Andreas, C.; En, T.C. Effect of pulsed electric current treatment on the corrosion and strength of reinforcing steel. *Mater. Sci. Forum* **2012**, *706*, 937–944.
16. Roh, J.-H.; Seo, J.-J.; Hong, S.-T.; Kim, M.-J.; Han, H.N.; Roth, J.T. The mechanical behavior of 5052-H32 aluminum alloys under a pulsed electric current. *Int. J. Plast.* **2014**, *58*, 84–99. [[CrossRef](#)]
17. Park, J.-W.; Jeong, H.-J.; Jin, S.-W.; Kim, M.-J.; Lee, K.; Kim, J.J.; Hong, S.-T.; Han, H.N. Effect of electric current on recrystallization kinetics in interstitial free steel and AZ31 magnesium alloy. *Mater. Charact.* **2017**, *133*, 70–76. [[CrossRef](#)]
18. Yang, C.; Lim, J.A.; Ding, Y.F.; Zhang, W.W.; Li, Y.Y.; Fu, Z.Q.; Chan, F.; Lavernia, E.J. Texture evolution and mechanical behavior of commercially pure Ti processed via pulsed electric current treatment. *J. Mater. Sci.* **2016**, *51*, 10608–10619. [[CrossRef](#)]
19. Yang, C.L.; Yang, H.J.; Zhang, Z.J.; Zhang, Z.F. Recovery of tensile properties of twinning-induced plasticity steel via electropulsing induced void healing. *Scr. Mater.* **2018**, *147*, 88–92. [[CrossRef](#)]
20. Harvey, D.P.; Jolles, M.I. Estimation of the yield strength of metals from crystal defect energies. *Metall. Trans. A* **1990**, *21*, 1719–1723. [[CrossRef](#)]
21. Qi, C.Z.; Xia, C.; Li, X.Z.; Sun, Y.J. Effect of inertia and crack propagation on dynamic strength of geologic-type. *Mater. Int. J. Impact Eng.* **2019**, *133*, 103367.
22. Yu, T.; Deng, D.W.; Wang, G.; Zhang, H.C. Crack healing in SUS304 stainless steel by electropulsing treatment. *J. Clean. Prod.* **2016**, *113*, 989–994. [[CrossRef](#)]
23. Kim, G.Y.; Ni, J.; Koc, M. Modeling of the size effects on the behavior of metals in microscale deformation processes. *J. Manuf. Sci. Eng.* **2007**, *129*, 470–476. [[CrossRef](#)]

24. Chan, W.L.; Fu, M.W. Experimental studies and numerical modeling of the specimen and grain size effects on the flow stress of sheet metal in microforming. *Mater. Sci. Eng. A* **2011**, *528*, 7674–7683. [[CrossRef](#)]
25. Liu, J.G.; Fu, M.W.; Lu, J.; Chan, W.L. Influence of size effect on the springback of sheet metal foils in micro-bending. *Comput. Mater. Sci.* **2011**, *50*, 2604–2614. [[CrossRef](#)]

Disclaimer/Publisher’s Note: The statements, opinions and data contained in all publications are solely those of the individual author(s) and contributor(s) and not of MDPI and/or the editor(s). MDPI and/or the editor(s) disclaim responsibility for any injury to people or property resulting from any ideas, methods, instructions or products referred to in the content.